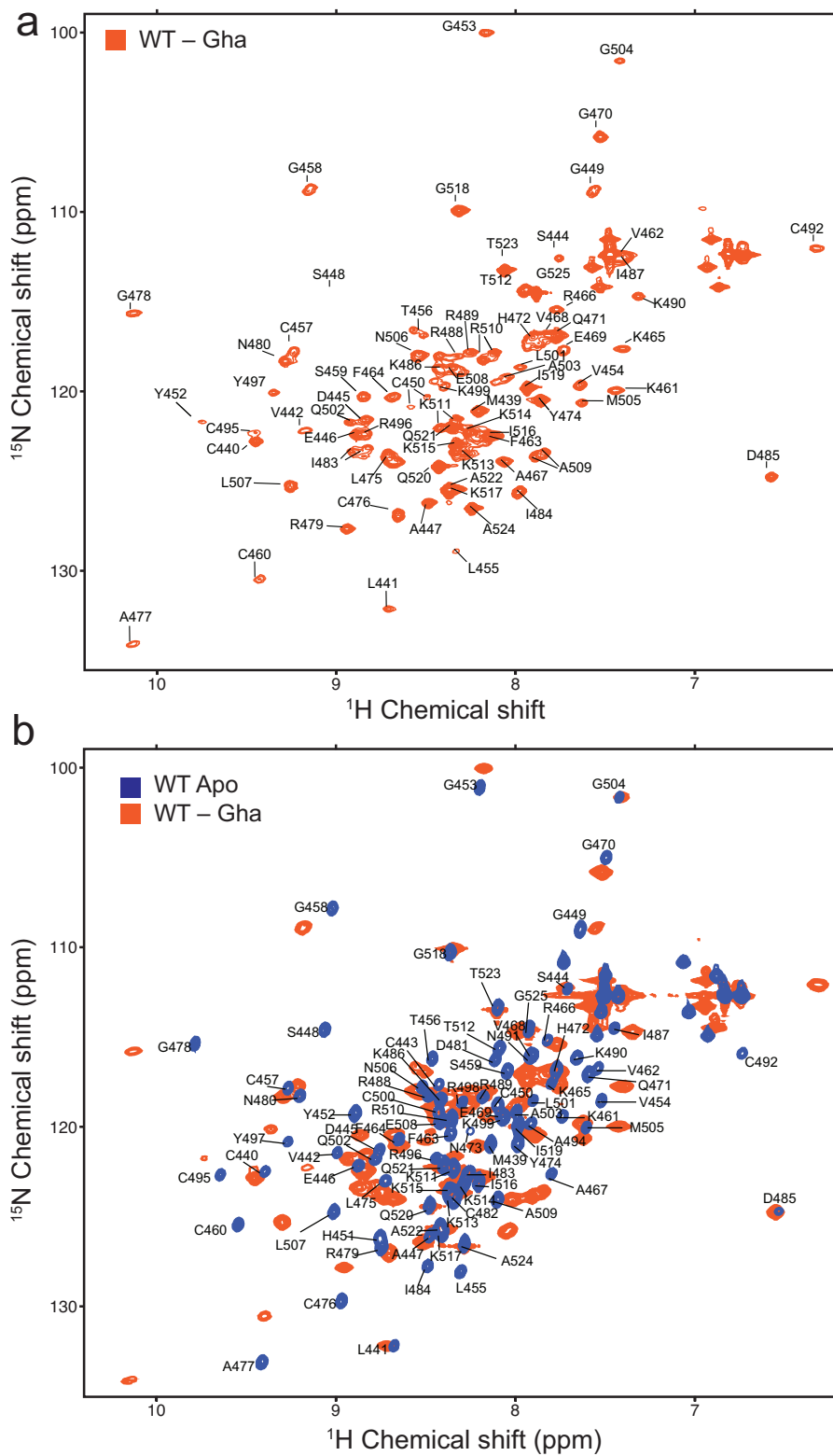


Supplementary Materials

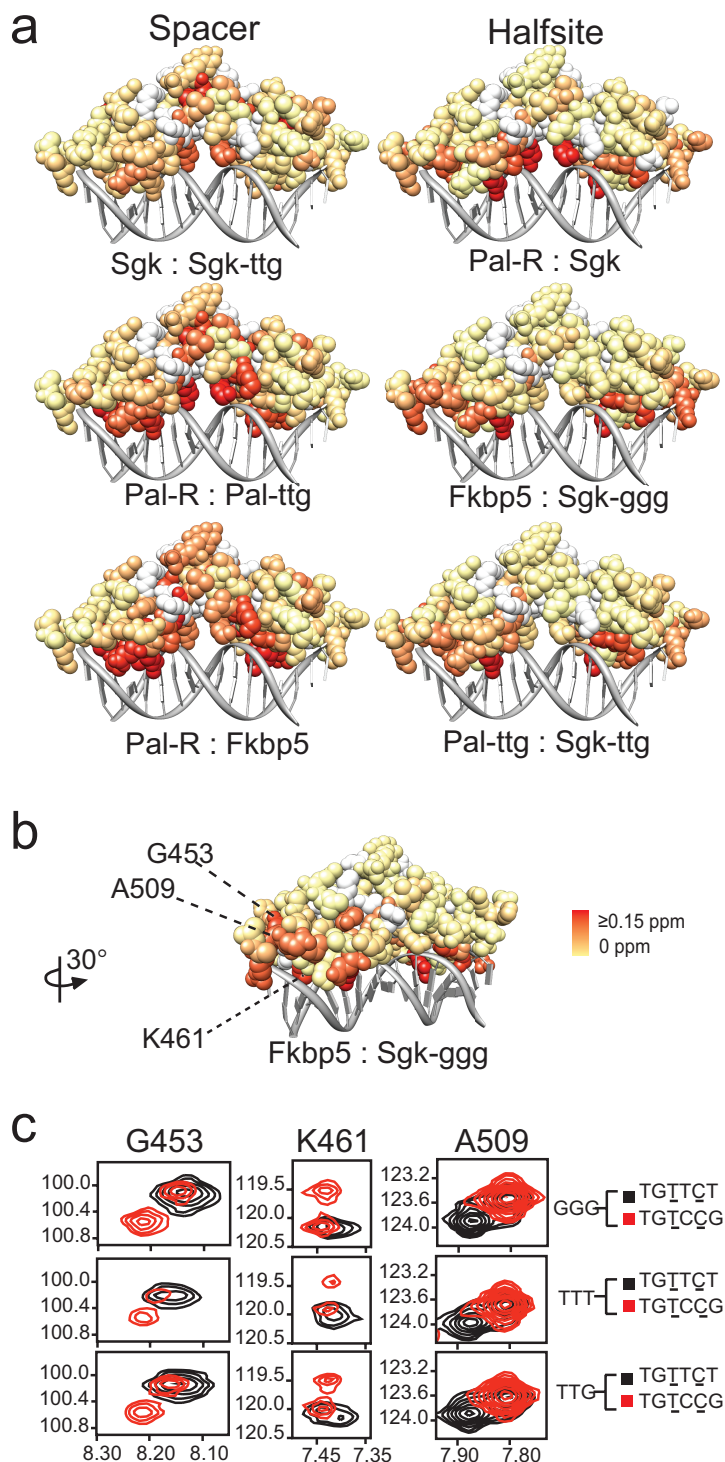
The glucocorticoid receptor dimer interface allosterically transmits sequence-specific DNA signals

Lisa C. Watson^{1,2}, Kristopher M. Kuchenbecker^{3,4}, Benjamin J. Schiller^{1,2}, John D. Gross⁵, Miles A. Pufall^{2,6}, Keith R. Yamamoto²

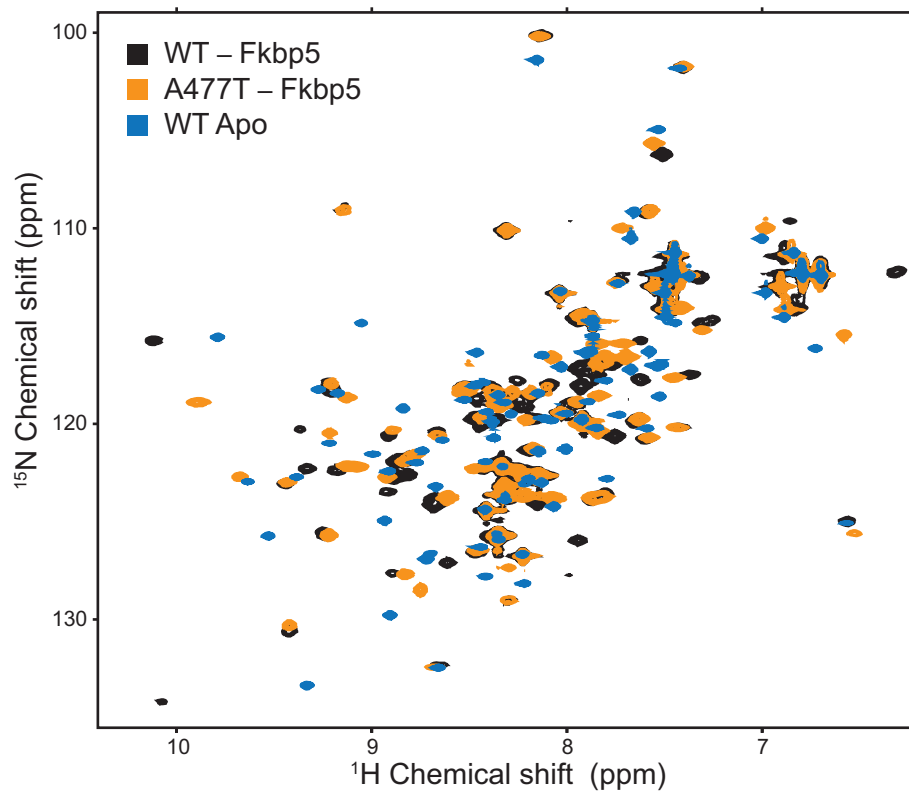
Supplementary Figure 1 NMR assignment of the DNA-bound GR DBD complex. (a) HSQC of $^2\text{H}^{15}\text{N}$ -labeled GR wild type (WT) DBD bound to the Gha GBS at 35°C. (b) Overlay of the ^{15}N -HSQC spectra of the unbound WT DBD (WT Apo) and WT DBD – Gha complex at 25°C.



Supplementary Figure 2 NMR chemical shift difference analysis of GBSs that differ in the half-site or spacer sequence. (a) Pairwise comparison of six GBS complexes showing the effect of changing either spacer or half-site positions 13 and 15 (half-site_{13:15}). NMR chemical shift differences are mapped on to the crystal structure of GR DBD (PDB ID:3g6u). (b) The locations within the GR DBD and (c) the overlay of ¹⁵N-HSQC peaks for residues that differ in half-site_{13:15}.

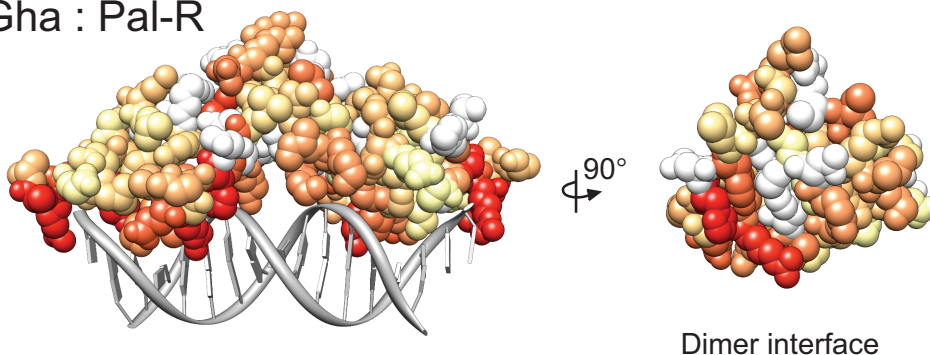


Supplementary Figure 3 DNA-bound A477T conformation differs from that of the unbound WT DBD. The overlay of ^{15}N -HSQC spectra of WT and A477T DBD bound to the Fkbp5 GBS, compared to the unbound DBD (WT Apo) at 35°C.

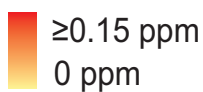
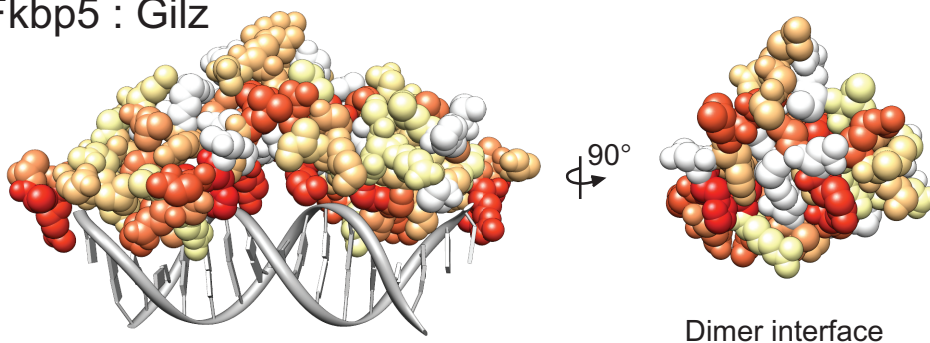


Supplementary Figure 4 Chemical shift difference between WT DBD – GBS complexes with different levels of transcriptional induction by GR. Structures are colored according to the magnitude of combined ^1H and ^{15}N NMR chemical shift differences for pairs of GBS complexes that have similar binding affinity, cooperativity and dissociation kinetics. Unassigned residues are colored white.

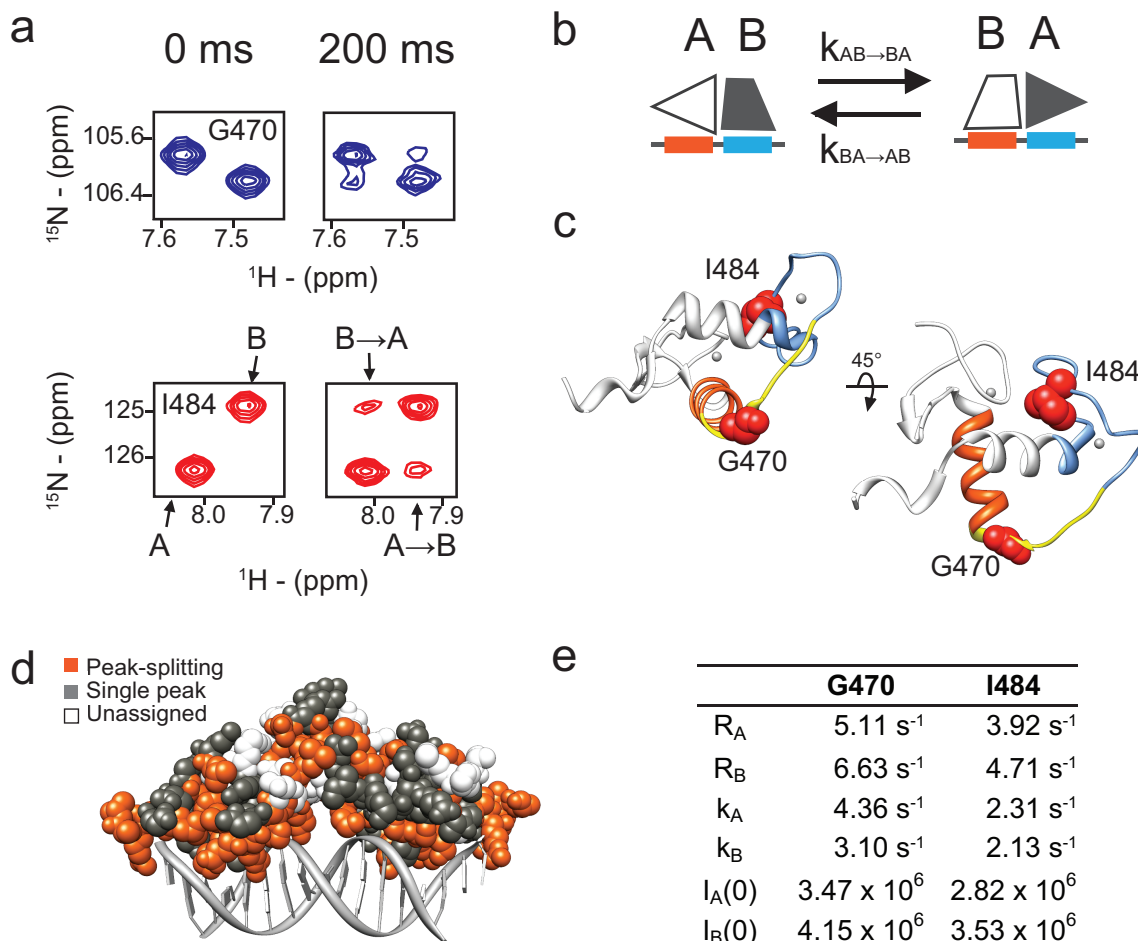
Gha : Pal-R



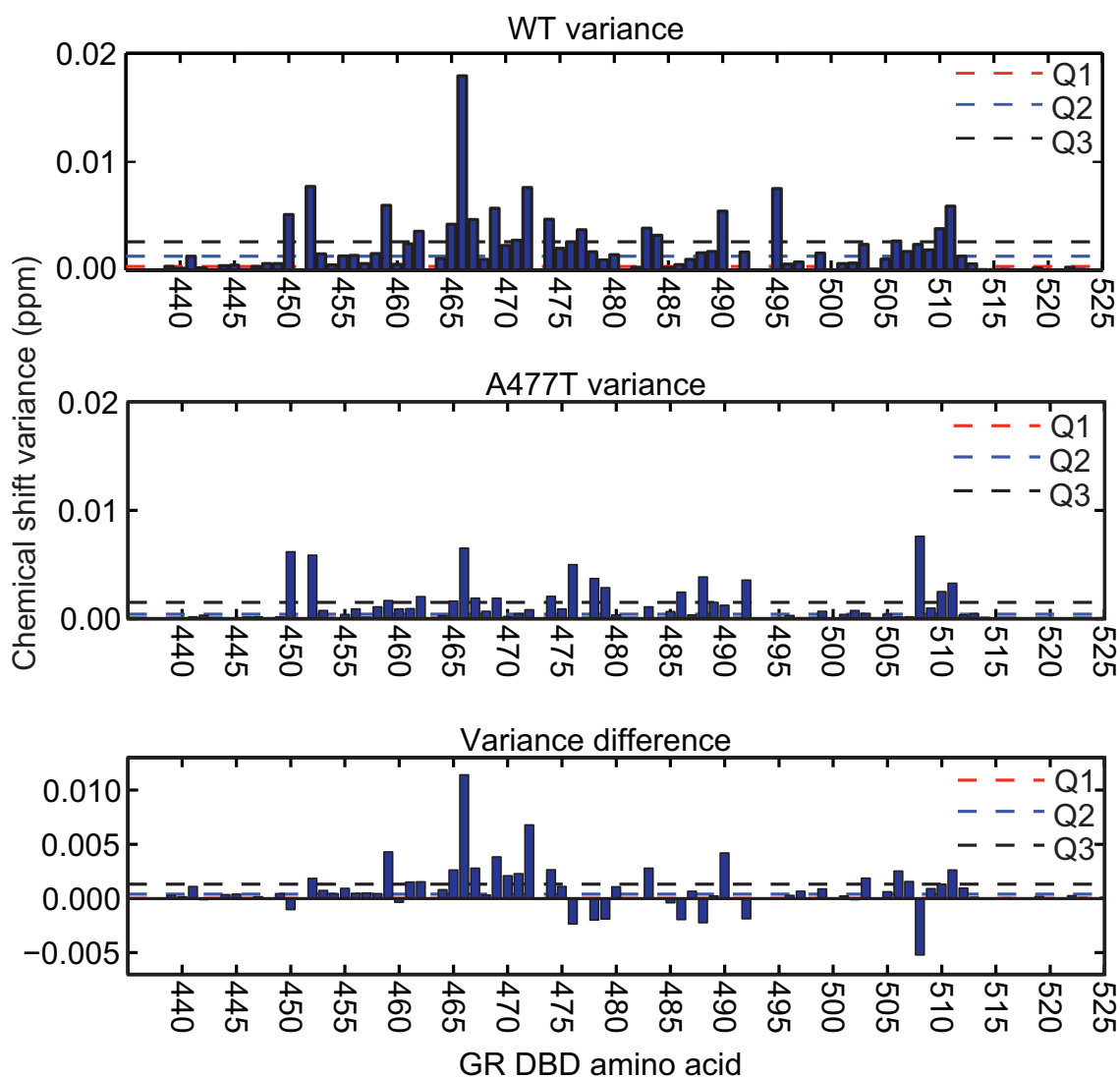
Fkbp5 : Gilz



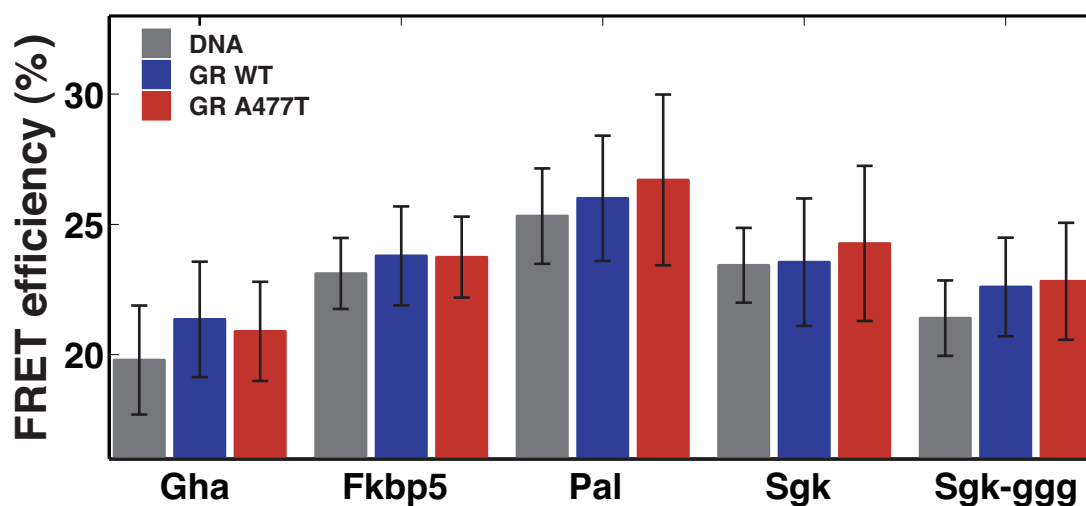
Supplementary Figure 5 Conformational exchange within the lever arm and dimer interface. (a) Zoomed view of ZZ-exchange NMR spectra for Gly470 and Ile484 with a 200 ms mixing period. The peaks indicate two conformational states, arbitrarily labeled A and B, at 0 ms mixing period and the exchange cross-peaks are labeled A→B and B→A. (b) Model for conformational swapping between dimer partners while bound to DNA, based on the observed rate of conformational exchange (k_A and k_B), which is faster than the measured GR dissociation rate from DNA (0.03 s^{-1}). (c) The location of Gly470 and Ile484 (red spheres) within the GR DBD monomer. Recognition helix (orange), lever arm (yellow), and zinc finger 2 of the dimer interface (light blue). (d) Mapping of ^{15}N -HSQC peaks of the WT DBD – Gilz complex that undergo peak-splitting from slow exchange. (e) The parameters from curves fit to ZZ-exchange peaks, where R = longitudinal relaxation rate of magnetization, k = exchange rate for converting from site A to B, and $I(0)$ = longitudinal magnetization at the start of the mixing period²⁷.



Supplementary Figure 6 NMR chemical shift variance across seven different GBS complexes. WT variance and A477T variance among ^{15}N -HSQC spectra for each amino acid calculated as σ_H^2 or $\sigma_N^2 = \sum(x - \mu)^2 / (n-1)$, where $x = ^1\text{H}$ or ^{15}N chemical shift (ppm), μ = the mean chemical shift (ppm), and $n = 7$; and combined as the variance sum: $\sigma_{NH}^2 = (1/5 \cdot \sigma_N^2) + \sigma_H^2$ (top and middle panel). The difference between WT and A477T chemical shift variance (bottom panel). The dotted lines represent the first quartile (Q1), median (Q2) the third quartile (Q3). Unassigned amino acids are plotted as zero.



Supplementary Figure 7 Comparison of sequence-specific DNA bend as determined by FRET assay. Alexa488 and Alexa546 fluorophores were conjugated to opposite 3' ends of 24-bp GBS-containing oligos, serving as the donor and acceptor, respectively. FRET was measured for five GBSs at 50 nM with and without GR DBD (500 nM WT or A477T). By assuming a bend at the center of the GBS, GR binding-induced DNA bend is less than 1° for all GBSs, using the formula $R = R_0[(1/E)-1]^{1/6}$, where R = distance, E = efficiency and R_0 = Förster distance of the FRET pair. All FRET assays were performed in NMR buffer using a Molecular Devices SpectraMax M5 with a fixed excitation of 444 nM and an emission scan from 500-650 nm. Equivalent results were obtained using 1 μ M protein, indicating saturated binding under these conditions. Data is shown as the mean \pm two s.d. from 12 replicates.



GBS	FRET Efficiency			p-value		
	DNA	WT	A477T	DNA vs. WT	DNA vs. A477T	WT vs. A477T
Gha	19.8 \pm 2.1	21.4 \pm 2.2	20.9 \pm 1.9	0.0018	0.0133	0.2873
Fkbp5	23.1 \pm 1.4	23.8 \pm 1.9	23.7 \pm 1.6	0.0576	0.0470	0.8929
Pal	25.3 \pm 1.8	26.0 \pm 2.4	26.7 \pm 3.3	0.1312	0.0177	0.2423
Sgk	23.4 \pm 1.4	23.6 \pm 2.4	24.3 \pm 3.0	0.7697	0.0917	0.2089
Sgk-ggg	21.4 \pm 1.4	22.6 \pm 1.9	22.8 \pm 2.2	0.0022	0.0013	0.6107

Supplementary Table 1 Summary of SPR fit parameters for WT and A477T DBD binding to GBS surfaces at 35°C or 8°C. Dissociation constant, $K_{1/2}$, and Hill coefficient, n_H , were calculated from equilibrium binding isotherms fit to a the Hill equation. Fitting of the dissociation phases of the SPR traces by conventional models gave systematic residuals consistent with a biphasic-sequential dissociation process, likely resulting from the complex kinetics and strong cooperativity of this system. Instead, the stabilities of the different complexes were reliably determined by a standard exponential decay model, and $t_{1/2}$ values were extrapolated from the apparent off-rates. Errors are the mean \pm two s.d. from 2-3 replicates.

GBS	WT			A477T		
	$K_{1/2}$ (nM)	n_H	$t_{1/2}$ (s)	$K_{1/2}$ (nM)	n_H	$t_{1/2}$ (s)
	35°C			35°C		
Pal-R	1.6 \pm 0.2	2.1 \pm 0.3	55 \pm 4	16 \pm 1	1.4 \pm 0.1	4.8 \pm 0.7
Gilz	5.7 \pm 0.6	1.8 \pm 0.3	23 \pm 2	28 \pm 1	1.3 \pm 0.2	4.7 \pm 0.8
	8°C			8°C		
Gha	2.7 \pm 0.2	2.2 \pm 0.2	160 \pm 20	21 \pm 1	1.2 \pm 0.05	18 \pm 1
Pal-R	3.1 \pm 0.1	2.1 \pm 0.1	120 \pm 20	39 \pm 1	0.9 \pm 0.03	13 \pm 0.8
Sgk	9.7 \pm 0.2	1.8 \pm 0.06	50 \pm 7	42 \pm 1	1.0 \pm 0.02	10 \pm 0.7
Fkbp5	12 \pm 0.2	2.0 \pm 0.06	22 \pm 3	55 \pm 1	1.4 \pm 0.02	5.9 \pm 0.5
Gilz	13 \pm 0.2	1.9 \pm 0.05	28 \pm 4	71 \pm 5	1.1 \pm 0.03	7.6 \pm 0.7
Sgk-ttg	13 \pm 0.8	2.3 \pm 0.2	34 \pm 2	48 \pm 17	1.4 \pm 0.02	12 \pm 0.7
Sgk-ggg	20 \pm 0.7	1.9 \pm 0.06	18 \pm 3	166 \pm 23	1.1 \pm 0.05	5.8 \pm 0.6

Supplementary Table 2 Correlation between transcriptional activity and DNA-binding affinity ($K_{1/2}$) or half-life ($t_{1/2}$). Correlations for WT and A477T were calculated for seven different GBS complexes. Because this relationship is expected to be non-linear²⁶, a statistical analysis with non-linear fitting of data are presented.

Analysis	Wildtype		A477T	
	$K_{1/2}$	$t_{1/2}$	$K_{1/2}$	$t_{1/2}$
R^2 (log transformed)	0.22	0.17	0.71	0.43
Pearson's (R^2)	0.31	0.06	0.44	0.54